Bulletin of the Seismological Society of America, Vol. 94, No. 6, pp. 2407–2413, December 2004

Constraints on the Source Parameters of the 26 January 2001 Bhuj, India, Earthquake from Satellite Images

by Vineet K. Gahalaut and Roland Bürgmann

Abstract The Bhuj earthquake of 26 January 2001 (M_w 7.6) was the largest intracontinental earthquake of the modern era of seismology. Field investigations did not provide any evidence of coseismic surface rupture or ground deformation due to primary faulting. We analyze pre- and postearthquake satellite images of the epicentral region to suggest that there was a significant change in the flooding pattern of the seasonal Rann of Kachchh lagoon after the 2001 and 2002 monsoons in the region of coseismic uplift. The maximum uplift is located about 15 km north of the reported epicenter and acted as a barrier against the northward draining rainwater runoff. Furthermore, the earthquake caused a northward shift in the southern limit of the Rann of Kachchh. We use this information to place constraints on the location and geometry of the earthquake rupture and suggest that the depth of the updip edge of the rupture is about 10 km.

Introduction

The 26 January 2001, Bhuj earthquake (M_w 7.6) occurred in the Rann of Kachchh region (Fig. 1). The geologic structures in the epicentral region evolved during a long history of tectonic activity that began in the Proterozoic and involved several major tectonic episodes that fragmented Gondwanaland during Mesozoic and Paleogene periods (Biswas, 1987; Merh, 1995; Talwani and Gangopadhyay, 2001; Hengesh and Lettis, 2002). In the late Triassic or early Jurassic, several smaller rift systems developed deep sedimentary basins, including the Kachchh basin. These structures were reactivated as a result of regional compression arising due to Indian plate movement in the Cenozoic. This is evident from the fold and thrust belt along the Kachchh mainland fault system and the Allah Bund fault (Malik *et al.*, 2000) and also by the occurrence of major reverse earthquakes in the past 200 years, namely, the 1819 Allah Bund (Bilham, 1998; Rajendran and Rajendran, 2001), the 1956 Anjar (Chung and Gao, 1995), and the 2001 Bhuj earthquakes (Fig. 1).

The 2001 Bhuj earthquake is the largest intracontinental earthquake of the modern seismological era. It occurred in the failed rift region on a steeply south-dipping reverse fault. Apart from being a large earthquake that caused a great loss of life and damage to property, a few aspects make this earthquake interesting. First, this region lies about 400 km east of the nearest plate boundary and thus strain rates are expected to be low (Stein *et al.*, 2002). However, an earthquake in 1819 (M $\sim$ 8) occurred only about 100 km northwest of the 2001 Bhuj earthquake epicenter (Bilham, 1998; Rajendran and Rajendran, 2001). Another event of moderate magnitude (M_w 6.0), known as the Anjar earthquake, occurred south of the recent earthquake (Fig. 1; Chung and Gao, 1995). In addition to the two major 1668 and 893 A.D. earthquakes, Rajendran and Rajendran (2001, 2002) reported 15 historic and recent earthquakes of M 5–6 from the region. Second, seismic studies of the coseismic rupture and its aftershocks suggest that the rupture area of the 2001 Bhuj earthquake was small, about 40×40 km^2 and consequently the static stress drop was large, 13 to 25 MPa on a deeply buried fault plane (Negishi *et al.*, 2002; Antolik and Dreger, 2003). Third, the earthquake occurred in the lower crust on a steeply dipping reverse fault, and the rupture did not extend up to the surface or project toward a mapped surface fault. Field investigations did not provide any evidence of coseismic rupture or land deformation due to primary faulting, which is unusual for such a large crustal earthquake. However, secondary features related to the earthquake, such as fractures, lateral spreads, soil liquefaction, and sand boils, were abundant in the meisoseismal area (Bendick *et al.*, 2001; Rajendran *et al.*, 2001; Singh *et al.*, 2001; Wesnousky *et al.*; 2001; Saraf *et al.*; 2002; Pinty *et al.*, 2003). Finally, although the earthquake occurred in the modern era of seismology, almost no near-field data are available for this event. The region is poorly instrumented and lies close to the international border of India with Pakistan. The most recent geodetic measurements in the region were undertaken during the Great Trigonometric Survey of India in 1856–1860 (Jade *et al.*, 2003) and there was no seismic network in place before the event. Unfortunately, problems in Synthetic Aperture Radar interferograms across the area have so far prevented the generation of remotely sensed deformation measurements.

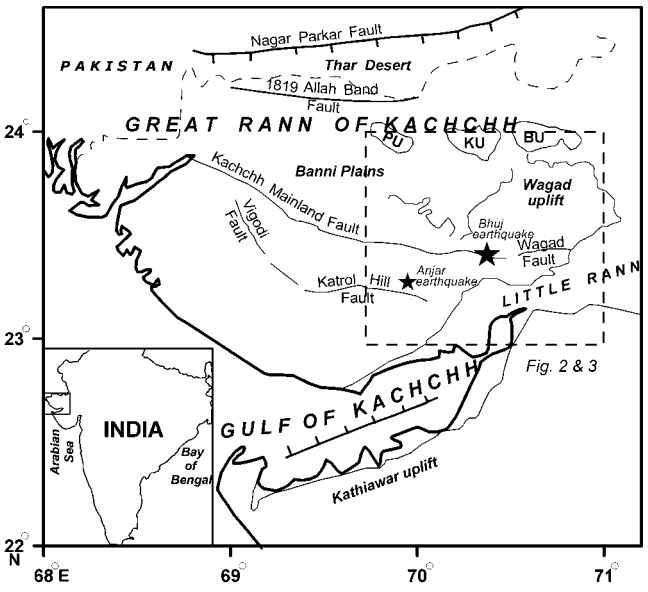

Figure 1. Generalized structural map of Kachchh (simplified after Biswas, 1987; Malik *et al.*, 2000). PU, Pachchham uplift; KU, Khader Uplift; BU, Bela Uplift. Location of images in Figures 2 and 3 is also indicated.

This earthquake could provide information about the deformation mechanisms, recurrence interval, and earthquake occurrence processes in other similar intracontinental regions of the world (e.g., the New Madrid region of the central United States or the Charleston region of eastern United States) and inputs to the seismic hazard estimation in such regions. However, in general, our knowledge about the source parameters of this earthquake is poor. In this article we focus on this aspect and compare satellite images of the region before and after the earthquake to infer geomorphological changes, which can be utilized to constrain source parameters of the earthquake.

Analysis of Satellite Imagery

We analyzed satellite imagery taken before and after the earthquake to detect changes in seasonal drainage and flooding patterns in the epicentral area that were caused by coseismic elevation changes. We evaluated about 100 images from the Landsat, Terra (using Advanced Spaceborne Thermal Emission and Reflection Radiometer [ASTER] sensor), Satellite Probatoire pour I'Observation de la Terre (SPOT), and the Indian Remote Sensing (IRS) spacecraft and also evaluated radar amplitude images of the European Remote Sensing (ERS) spacecraft. The Terra acquisitions did not have sufficient spatial and temporal coverage of the region. Landsat images from October 1999 to September 2002, for which cloud cover was 30% or less, and IRS-1D (using Liss3 sensor) images from March 1999 to October 2002 were analyzed. We compared the pre- and postearthquake images that were taken after the monsoon period and compared low-lying regions that experience seasonal flooding, particularly in the southernmost Rann of Kachchh (Fig. 2). Topographic maps with limited benchmark elevation data and a recently released 3- arcsecond digital elevation model of the area based on data collected by the Shuttle Radar Topography Mission (SRTM) in February of 2000 (Fig. 3a) show that the area is very flat with a gentle northward slope. Across the area, seasonal overland flow drains the hills to the south. We found that prior to the Bhuj earthquake, flooding after the monsoon occurred in a region between latitudes 23.45 and 23.55° N and longitudes 70.23 to 70.30° E, as seen in the postmonsoon images of the years 1999 and 2000 (Fig. 2a–d). There were no indications of flooding in the region lying immediately south of it. In the postearthquake, postmonsoon images (Fig. 2e–i), we find that the region southwest of the region of previous flooding experienced ponding in a large area. About 15 km west-northwest of the reported U.S. Geological Survey (USGS) epicenter, flooding of an area of about 50 km^2, at latitudes 23.39 to 23.46° N and longitudes 70.12 to 70.27° E, occurred in the postearthquake monsoon period, whereas prior to 2001, namely in 1999 and 2000, flooding occurred farther north of this region (Fig. 2). This new pattern of flooding is also apparent in the postmonsoon images of the year 2002 (Fig. 2i). It appears that the region of postearthquake flooding subsided relative to the region that experienced flooding during pre-earthquake years. The southern limit of the flooded portion of the main Rann of Kachchh shifted northward by about 10 km (see dashed line indicating the postseismic seasonal shoreline in Fig. 2). These two observations document that relative uplift occurred in a ~20-km-wide zone between latitudes 23.40 and 23.60° N.

Interpretation and Discussion

To interpret the apparent uplift pattern, we use elastic dislocation theory (Mansinha and Smylie, 1971) to calculate the coseismic elevation changes, assuming uniform slip that tapers at the edges of the rupture. Several focal mechanism solutions are reported (Wesnousky *et al.*, 2002) that all suggest predominantly reverse motion on a steeply south dipping (51–66°) fault. Antolik and Dreger (2003) reported a focal mechanism solution on the basis of far-field waveform modeling. We used their focal mechanism solution as a starting model in our analysis (NP1: 82°, 51°, 77°). As expected, the predicted elevation changes indicate uplift in the hanging wall, in the south, and subsidence in the footwall, in the north. We used aftershock data of this earthquake (Negishi *et al.*, 2002) to define the geographical location and size of the rupture. From the aftershock data, it appears that the rupture had an approximate along-strike length of about 40 km and extended to as much as a 37- to 39-km depth. Although there are few aftershocks at shallow depths, these data are unable to place any firm constraints on the updip edge of the rupture.

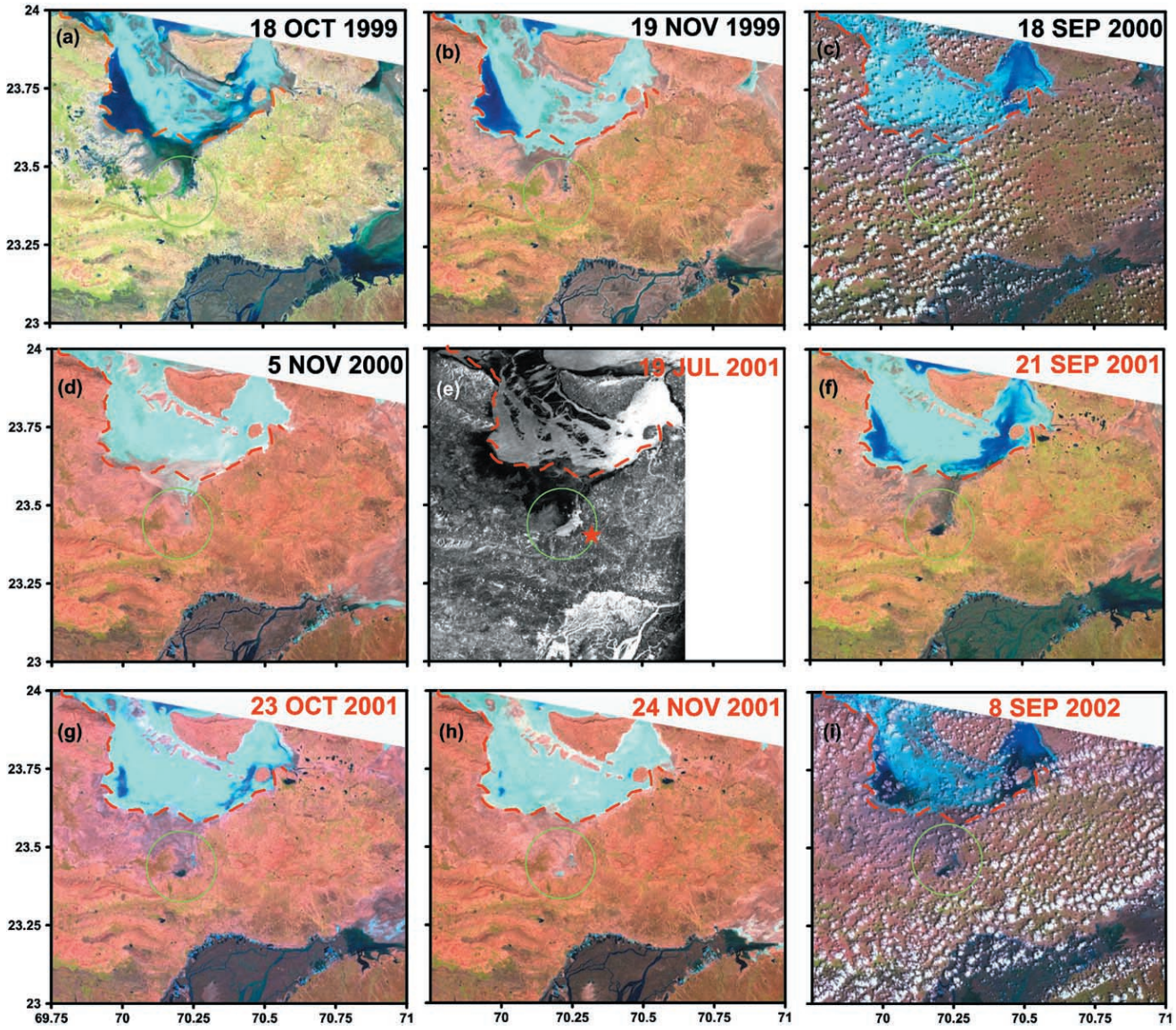

Figure 2. Pre- (a–d) and post- (e–i) earthquake images (colored are Landsat and black-and-white are ERS images), after the monsoon period. The dates of images are indicated in each panel. The red dashed curve marks the postearthquake southern limit of the flat salt region. In the pre-earthquake images the limit of the seasonally flooded salt region extends south of the postearthquake limit. Green circle indicates the region of flooding in the postearthquake periods. Star in the ERS image indicates the 2001 Bhuj earthquake epicenter.

Figure 3b shows the predicted elevation changes due to the considered rupture, with an updip edge at 10 km depth and slip of 5 m. Uplift is predicted over a wide region above the aftershocks. There is subsidence in the low-lying flat salt region in the north that lies between the islands formed by Pachham and Khadir uplift (Fig. 1). The model predicts maximum coseismic uplift of $\geq$2 m at about 23.45° N, in the region that used to be seasonally flooded in the pre-earthquake monsoon periods. Thus, we suggest that this uplift caused a reversal in slope and acted as a barrier to run off, causing flooding to the south (Fig. 4). The uplift also shifted northward the southern limit of the flooded salt land, while the flooding elsewhere reached levels comparable with previous years (Fig. 2).

The location of the postseismically flooded region and the 20-km distance between this region and the coseismic subsidence in the north may be used to provide additional constraints on the location and depth of the rupture. As noted above, topographic information about the Rann of Kachchh from published maps and the SRTM data show that the area in which flooding occurred is flat with a very gently northward slope (Fig. 3a). The northward shift of $\sim$10 km in the

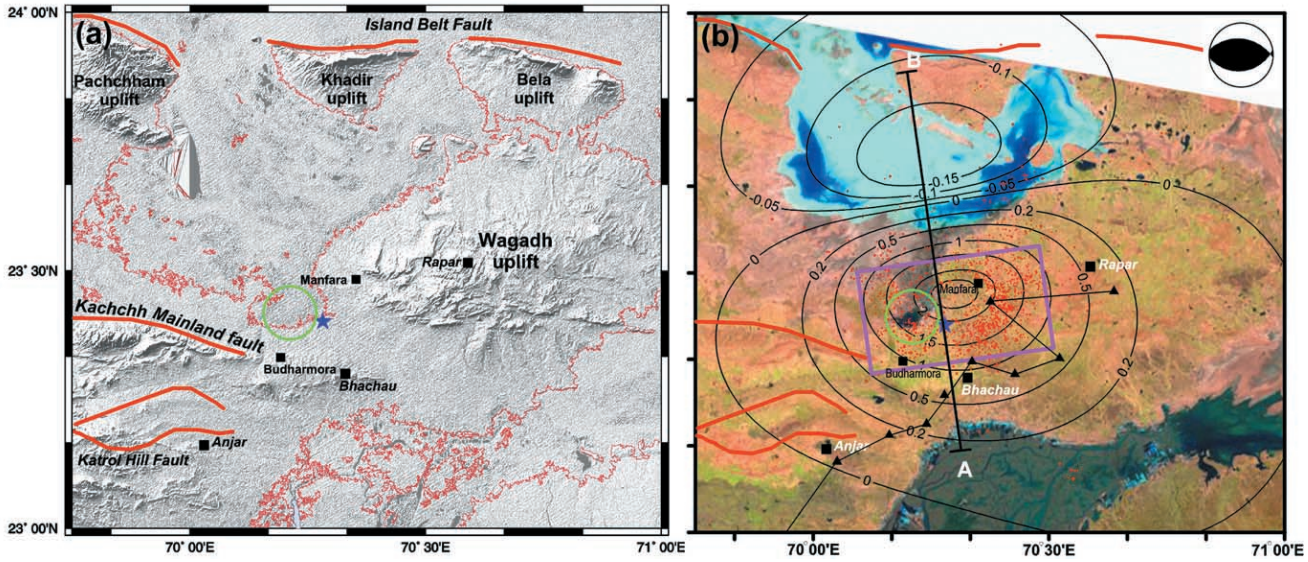

Figure 3. (a) Digital elevation model of the region generated by the data collected by Shuttle Radar Topography Mission (SRTM) with contours of 5 m. Bhuj earthquake epicenter (star) and the identified region of postseismic flooding (green circle) are also indicated. Note the flatness and low elevation of the region lying between Pachchham Uplift, Khadir uplift, and the epicentre. (b) Coseismic elevation changes, (note the nonuniform contour interval in meters) from slip of 5 m, on a 51° S dipping, 40-km-wide rupture, with updip and downdip edges at 10 and 37 km, respectively. The projected dislocation plane (pink rectangle), the epicenter of aftershocks (red dots; Negishi *et al.*, 2002), the mainshock epicenter (star), and the fault-plane solution (Antolik and Dreger, 2003) are all shown on the Landsat image of 21 September 2001. The bluish-black region, shown within the green circle, that lies west of the mainshock epicenter, is the identified region of postseismic flooding. Faults are drawn after Malik *et al.* (2000). Triangles denote the benchmarks of the leveling surveys done during 1997–1999, before the earthquake, and during November 2001, after the earthquake (Chandrasekhar *et al.*, 2004). Line A–B shows the profile of elevation changes in Figures 4 and 5.

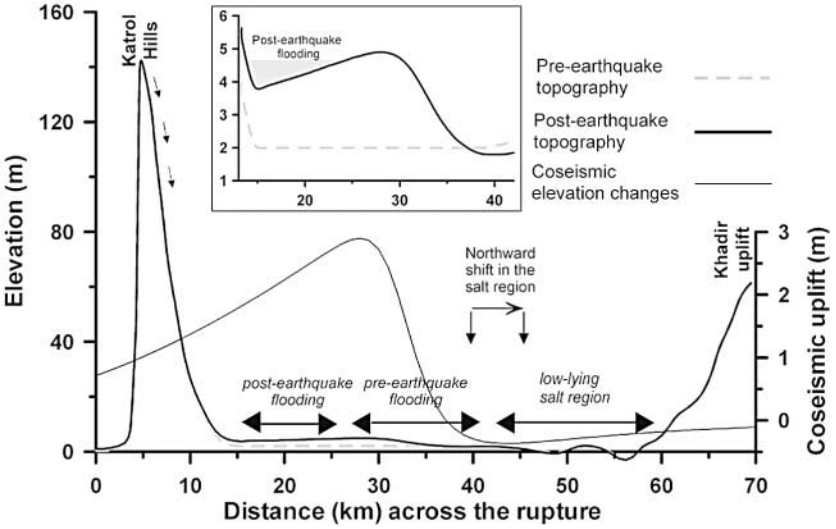

Figure 4. A cross section showing how flooding occurred after the earthquake. Coseismic elevation changes (scale to the right), preearthquake topography from SRTM data, and postearthquake topography (scale to the left) are shown along the line A–B of Figure 3. Inset shows the highly vertically exaggerated pre- and postearthquake topography of the region of postearthquake flooding and demonstrates the cause of flooding in the region south of the region of maximum coseismic uplift.

southern limit of the Rann of Kachchh (Fig. 2) and relative coseismic uplift of about 1 m between the region of pre- and postearthquake southern limits of the Rann of Kachchh (Fig. 3b) loosely constrain the northward slope of the region to be about 0.01%. Figure 4 suggests that flooding in the gently northward sloping area can occur only when the region of maximum coseismic uplift lies north of the region of postseismic flooding. In Fig. 5a, we vary the depth of the updip edge of the rupture from 0 to 20 km with an interval of 5 km and calculate the elevation changes across the rupture.

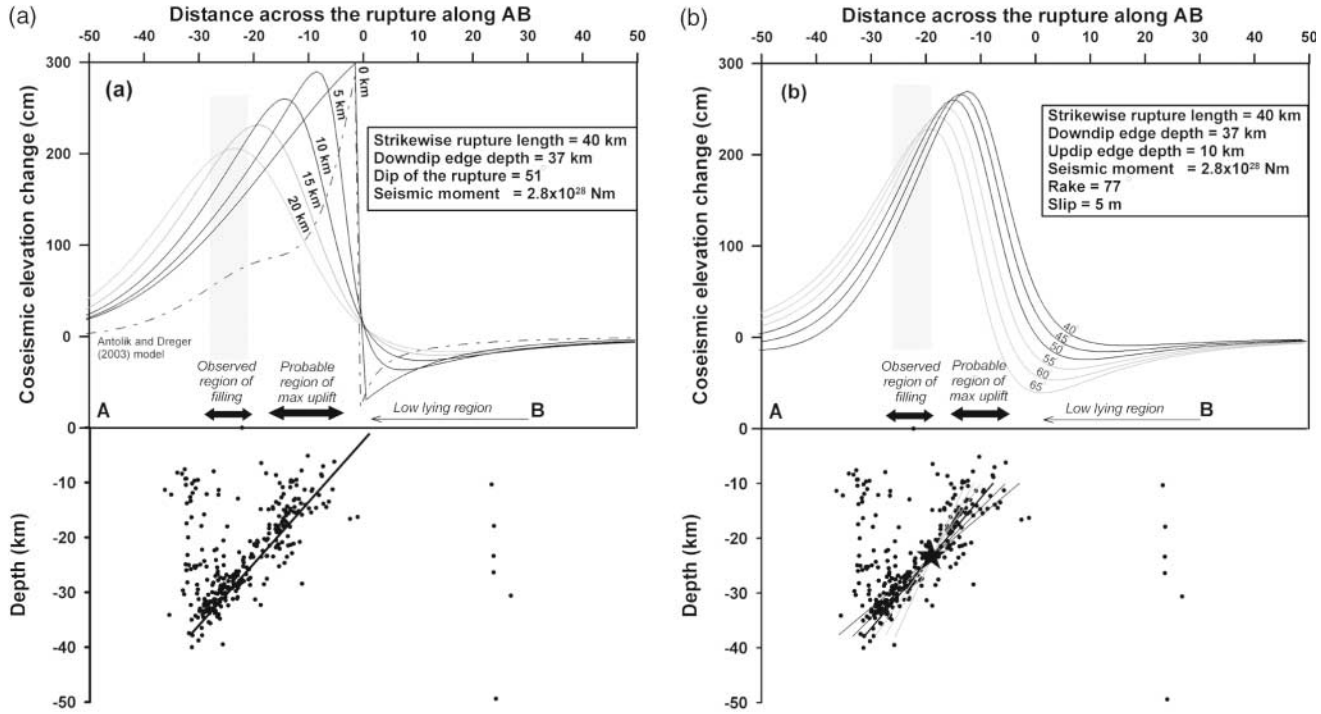

Figure 5. (a) Upper panel shows the variation of elevation changes along profile A–B with the change in depth of the upper edge of the rupture. Lower panel shows the depth cross section across AB and the aftershock distribution. Depth shallower than 10 km is consistent with the flooding in the region south of the maximum coseismic uplift. Elevation changes corresponding to Antolik and Dreger (2003) model are also shown in the upper panel. (b) Same as a, showing variation of elevation changes along profile A–B with the change in dip of the rupture. Lower panel shows the depth cross section across AB and the aftershock distribution. Dip of about 50° is generally consistent with the analysis.

All the other parameters are held constant, except the slip, which we vary to maintain the total moment of the earthquake to be constant. It can be seen that varying the depth of the rupture leads to a significant shift in the region of maximum uplift, but the region of subsidence does not shift significantly. Figures 4 and 5a suggest that the updip edge of the rupture may not lie deeper than 10 km, because a deeper updip edge will produce uplift either in the region of flooding or south of it. In fact, the coseismic uplift corresponding to a deeper updip edge of the rupture may not be enough to reverse the steep slope to cause flooding. Flooding can only occur in the gently sloping region as the contribution of coseismic elevation changes are not large compared with the topography in the adjacent higher regions to the west and east.

Antolik and Dreger (2003) suggested significant slip at depths less than 5 km. We argue against significant shallow slip, because (1) a shallow rupture should produce flooding to the north of the region of observed flooding, (2) their slip model does not produce uplift consistent with the region of flooding (Fig. 5a), and (3) the field investigations did not report any surface rupture for this earthquake. The variation in dip from 50 to 65° (Fig. 5b) does not greatly affect the elevation-change profile and hence we cannot further constrain the dip of the rupture plane. However a dip of 51° is the most consistent with the observations. Our estimate of uniform slip of 5 m may be considered a lower bound, because lower slip values would not be able to reverse the slopes. The estimated slip and coseismic elevation changes are consistent with those derived from repeat leveling observations (Fig. 3b; Chandrasekhar *et al.*, 2004), the Great Triangulation Survey and Global Positioning System measurements (Jade *et al.*, 2003), and teleseismic waveform modeling (Antolik and Dreger, 2003).

The dislocation model predicts subsidence in the north, which coincides with the low-lying flat region between the Pachham and Khadir islands. This apparent correlation between the earthquake-induced subsidence and the low-lying area suggests that similar large earthquakes in this region may have occurred in the past and contributed to the local topography. Unfortunately, no paleoseismological, subsurface geologic data are available to further support the previously stated inference. Further, ongoing erosion and deposition may also contribute to shaping the present land surface.

We emphasize that the changes in flooding patterns are not merely due to change in monsoon intensity or to earthquake-induced secondary features. From the extent of filling

in the Rann (Fig. 2) and record of rainfall of 432 mm at Bhuj station (India Meteorological Department; Pune, personal comm., 2003), it appears that the monsoon was very intense during 1999, but no flooding was observed in the region of postseismic flooding. Although the postearthquake imagery (e.g., Singh *et al.*, 2001) shows that liquefaction and some ground disturbances were quite broadly distributed and included our area of interest, we suggest that the regional pattern of changes in the Rann coastline and flooding to the south are more likely due to the earthquake-induced surface uplift. Moreover, the secondary features are not likely to produce flooding in such a large region that persists even after two monsoon seasons.

Conclusions

We analyzed the monsoonal flooding patterns in satellite imagery collected by Landsat, Terra, ERS, and IRS-1D in the years before and after the earthquake. It appears that about 15 km west-northwest of the reported USGS epicenter, flooding of an area of about 50 km^2 occurred in the ensuing monsoon period, whereas, prior to 2001, namely in 1999 and 2000, flooding occurred only further north of this region. The observed postearthquake changes in the distribution of flooding are consistent with a zone of maximum uplift near 23.45 to 23.55° N latitudes. The inferred uplift puts additional constraints on the location of the rupture. A rupture model with slip on a 40 $\times$ 40 km^2 rupture, extending from a depth of about 37 km to 10 km is consistent with the models suggested previously from teleseismic waveform inversions and the aftershock distribution. However, the model does not allow for significant slip at shallower depths, as proposed by Antolik and Dreger (2003). The dislocation model predicts subsidence in the north, which coincides with the low-lying salt flat region between the Pachham and Khadir islands. This apparent correlation between the earthquake-induced subsidence and the low-lying topography suggests that similar large earthquakes in this region may have occurred in the past.

Acknowledgments

V.K.G. acknowledges the financial support of Department of Science Technology through BOYSCAST fellowship to U.S.A. R.B. acknowledges European Space Agency Data Grant (AO3-330) for European Remote Sensing imagery. Steve Wesnousky suggested that we look at satellite images for inferring change in landform. We benefited from comments by Kusala Rajendran and Lorraine W. Wolf. Berkeley Seismological Laboratory Contribution 04-08.

References

Antolik, M., and D. S. Dreger (2003). Rupture process of the 26 January 2001 Mw 7.6 Bhuj, India, earthquake from teleseismic broadband data, *Bull. Seism. Soc. Am.* **93,** 1235–1248.

Bendick, R., R. Bilham, E. Fielding, V. K. Gaur, S. E. Hough, G. Kier, M. N. Kulkarni, S. Martin, K. Mueller, and M. Mukul (2001). The 26 January 2001 "Republic Day" earthquake, India, *Seism. Res. Lett.* **72,** 328–335.

Bilham, R (1998). Slip parameters for the Rann of Kuchchh, India, 16 June 1819, earthquake, quantified from contemporary accounts, in *Coastal Tectonics*, I. S. Stewart and C. Vita-Finzi (Editors), Geological Society London Special Publication, **146,** 295–319.

Biswas, S. K. (1987). Regional tectonic framework, structure and evolution of the western marginal basins of India, *Tectonophysics* **135,** 302–327.

Chandrasekhar, D. V., D. C. Mishra, B. Singh, V. Vijayakumar, and R. Bürgmann (2004). Source parameters of the Bhuj earthquake, India of January 26, 2001 from height and gravity changes, *Geophys. Res. Lett.* **31,** L19608, doi: 10.1029/2004GL020768.

Chung, W. Y., and H. Gao (1995). Source parameters of the Anjar earthquake of July 21, 1956, India and its seismotectonics implications for the Kutch rift basins, *Tectonophysics* **242,** 281–292.

Hengesh, J. V., and W. R. Lettis (2002). Geologic and tectonic setting, in Bhuj, India earthquake pf January 26, 2001 Reconnaissance report, S. K. Jain, W. R. Lettis, C. V. R. Murty, and J.-P. Bardet (Editors) *Earthquake Spectra* **18A,** 7–22.

Jade, S., M. Mukul, I. A. Parvez, M. B. Ananda, P. D. Kumar, V. K. Gaur, R. Bendick, R. Bilham, F. Blume, K. Wallace, I. A. Abbasi, M. A. Khan, and S. Ulhadi (2003) Preseismic, coseismic and post-seismic displacements associated with the Bhuj 2001 earthquake derived from recent and historic geodetic data, *Proceedings of Indian Academy of Science (Earth and Planetary Science)* **112,** 331–345.

Malik, J. N., P. S. Sohoni, S. S. Merh, and R. V. Karanth (2000). Paleoseismology and Neotectonism of Kachchh western India, in *Active Fault Research for the New Millennium, Proceedings of the Hokudan International Symposium and School of Active Faulting*, 251–259.

Mansinha, L., and D. E. Smylie (1971). Displacement fields of inclined faults, *Bull. Seism. Soc. Am.* **61,** 1433–1440.

Merh, S. S. (1995). *Geology of Gujrat*, Geological Society of India, Bangalore, India, 222 pp.

Negishi, H., J. Mori, T. Sato, R. Singh, S. Kumar, and N. Hirata (2002). Size and orientation of the fault plane for the 2001 Gujrat, India earthquake (Mw 7.7) from aftershock observations: a high stress drop event, *Geophys. Res. Lett.* **29,** 1949, doi: 10.1029/2002GL015280.

Pinty, B., N. Gorbon, M. M. Verstraete, F. Melin, Y. G. Widlowski, D. J. Diner, E. Fielding, D. L. Nelson, R. Madariaga, and M. P. Tuttle (2003). Observing earthquake related dewatering using MISR/Terra satellite data, *EOS Trans.* **84,** 37, 43.

Rajendran, C. P., and K. Rajendran (2001). Characteristics of deformation and past seismicity associated with the 1819 Kutch Earthquake, Northwestern India, *Bull. Seism. Soc. Am.* **91,** 407–426.

Rajendran, C. P., and K. Rajendran (2002). Historical constraints on previous seismic activity and morphologic changes near the source zone of the 1819 Rann of Kachchh earthquake: further light on the penultimate event, *Seism. Res. Lett.* **73,** 470–479.

Rajendran, K, C. P. Rajendran, M. Thakker, and M. P. Tuttle (2001). The 2001 Kutch (Bhuj) earthquake: coseismic surface features and their significance, *Curr. Sci.* **80,** 1397–1405.

Saraf, A. K., A. Sinvhal, H. Sinvhal, A. Ghosh, and B. Sarma (2002). Satellite data reveals 26 January 2001 Kutch earthquake-induced ground changes and appearance of water bodies, *Int. J. Remote Sensing* **23,** 1749–1756.

Singh, R. P., S. Bhoi, A. K. Sahoo, U. Raj, and S. Ravindran (2001). Surface manifestations after the Gujrat earthquake, *Curr. Sci.* **81,** 164–166.

Stein, S., G. Sella, and E. A. Okal (2002). The January 26, 2001, Bhuj earthquake and the diffuse western boundary of the Indian plate, in *Plate Boundary Zones*, S. Stein and J. T. Freymueller (Editors), 243–254.

Talwani, P., and A. Gangopadhyay (2001). Tectonic framework of the Kachchh earthquake of January 26, 2001, *Seism. Res. Lett.* **72,** 336–345.

Wesnousky, S. G., L. Seeber, T. Rockwell, V. Thakur, R. Briggs, S. Kumar, and D. Ragona (2001). Eight days in Bhuj: field report bearing on

surface rupture and genesis of the 26 January 2001 Republic Day earthquake of India, *Seism. Res. Lett.* **72,** 514–524.

National Geophysical Research Institute
Uppal Road, Hyderabad 50007
India
vkgahalaut@yahoo.com
(V.K.G.)

Department of Earth and Planetary Sciences and Berkeley Seismological Laboratory
University of California
Berkeley, California 94720-4760
burgmann@seismo.berkeley.edu
(R.B.)

Manuscript received 23 February 2004.